

# Final results of experiment to search for $2\beta$ processes in zinc and tungsten with the help of radiopure $\text{ZnWO}_4$ crystal scintillators

P. Belli<sup>1</sup>, R. Bernabei<sup>1,2,†</sup>, F. Cappella<sup>3,4</sup>, R. Cerulli<sup>5</sup>,  
 F.A. Danevich<sup>6</sup>, S. d'Angelo<sup>1,2</sup>, A. Incicchitti<sup>3,4</sup>,  
 V.V. Kobychev<sup>6</sup>, D.V. Poda<sup>5,6</sup>, V.I. Tretyak<sup>6</sup>

<sup>1</sup> INFN sezione Roma “Tor Vergata”, I-00133 Rome, Italy

<sup>2</sup> Dipartimento di Fisica, Università di Roma “Tor Vergata”, I-00133, Rome, Italy

<sup>3</sup> INFN sezione Roma “La Sapienza”, I-00185 Rome, Italy

<sup>4</sup> Dipartimento di Fisica, Università di Roma “La Sapienza”, I-00185 Rome, Italy

<sup>5</sup> INFN, Laboratori Nazionali del Gran Sasso, I-67100 Assergi (AQ), Italy

<sup>6</sup> Institute for Nuclear Research, MSP 03680 Kyiv, Ukraine

## Abstract.

A search for the double beta decay of zinc and tungsten isotopes has been performed with the help of radiopure  $\text{ZnWO}_4$  crystal scintillators (0.1 – 0.7 kg) at the Gran Sasso National Laboratories of the INFN. The total exposure of the low background measurements is  $0.529 \text{ kg} \times \text{yr}$ . New improved half-life limits on the double beta decay modes of  $^{64}\text{Zn}$ ,  $^{70}\text{Zn}$ ,  $^{180}\text{W}$ , and  $^{186}\text{W}$  have been established at the level of  $10^{18} - 10^{21} \text{ yr}$ . In particular, limits on double electron capture and electron capture with positron emission in  $^{64}\text{Zn}$  have been set:  $T_{1/2}^{2\nu 2K} \geq 1.1 \times 10^{19} \text{ yr}$ ,  $T_{1/2}^{0\nu 2\varepsilon} \geq 3.2 \times 10^{20} \text{ yr}$ ,  $T_{1/2}^{2\nu\varepsilon\beta^+} \geq 9.4 \times 10^{20} \text{ yr}$ , and  $T_{1/2}^{0\nu\varepsilon\beta^+} \geq 8.5 \times 10^{20} \text{ yr}$ , all at 90% C.L. Resonant neutrinoless double electron capture in  $^{180}\text{W}$  has been restricted on the level of  $T_{1/2}^{0\nu 2\varepsilon} \geq 1.3 \times 10^{18} \text{ yr}$ . A new half-life limit on  $\alpha$  transition of  $^{183}\text{W}$  to the metastable excited level  $1/2^-$  375 keV of  $^{179}\text{Hf}$  has been established:  $T_{1/2} \geq 6.7 \times 10^{20} \text{ yr}$ .

PACS numbers: 29.40.Mc, 23.40.-s

*Keywords:* Double beta decay. Radioactivity  $^{64}\text{Zn}$  ( $2\varepsilon$ ,  $\varepsilon\beta^+$ ).  $^{70}\text{Zn}$  ( $2\beta^-$ ).  $^{180}\text{W}$  ( $2\varepsilon$ ).  $^{186}\text{W}$  ( $2\beta^-$ ).  $\text{ZnWO}_4$  crystal scintillators. Low background experiment

† Corresponding author. E-mail: rita.bernabei@roma2.infn.it

## 1. Introduction

Double beta ( $2\beta$ ) processes are nuclear transformations when the charge of nuclei changes by two units:  $(A, Z) \rightarrow (A, Z \pm 2)$ . There are two main modes of  $2\beta$  decay: two neutrino mode ( $2\nu$ ) when two neutrinos are emitted together with two beta particles, and neutrinoless mode ( $0\nu$ ).  $0\nu 2\beta$  decay violates the lepton number by two units and therefore is forbidden in the Standard Model (SM) [1]. However, the  $0\nu 2\beta$  decay is predicted in some SM extensions where neutrino is expected to be a true neutral particle equivalent to its antiparticle (Majorana particle) [2]. Experiments on neutrino oscillations already gave evidence for neutrino to be massive [3], however these experiments are sensitive only to the differences of squared masses of neutrinos. The observation of  $0\nu 2\beta$  decay could resolve important problems of particle physics: what is the absolute scale of neutrino mass? Which neutrino mass hierarchy (normal, inverted, or quasi-degenerate) is realized in nature? Is the neutrino Majorana ( $\nu = \bar{\nu}$ ) or Dirac ( $\nu \neq \bar{\nu}$ ) particle? Is the lepton number absolutely conserved? Additionally, investigations of neutrinoless double  $\beta$  decay could test admixture of right-handed currents in electroweak interaction and existence of majorons§.

While  $2\nu 2\beta$  decay is allowed in the SM, it is a second order process in perturbation theory characterized by extremely low probability. Investigations of the  $2\nu 2\beta$  decay examine theoretical calculations of the nuclear matrix elements, contributing to the development of theoretical description of  $0\nu 2\beta$  decay.

Double beta decay experiments are concentrated mainly on  $2\beta$  processes with emission of two electrons ( $2\beta^-$ ). Two neutrino mode of  $2\beta^-$  decay was detected for 11 nuclides among 35 candidates; corresponding half-lives are in the range of  $10^{18} - 10^{24}$  yr [9, 10, 11, 12]. In addition, the  $2\nu 2\beta^-$  transitions of  $^{100}\text{Mo}$  and  $^{150}\text{Nd}$  to the first  $0^+$  excited states of daughter nuclei were observed too [9, 10, 11]. To-date the  $2\nu 2\beta^-$  decay is the rarest radioactive decay ever discovered. Developments in the experimental techniques during last two decades lead to impressive improvement of sensitivity to the neutrinoless mode of  $2\beta^-$  decay up to the level of  $T_{1/2} \sim 10^{23} - 10^{25}$  yr [9, 11]. Moreover, some possible positive indication for  $^{76}\text{Ge}$  with  $T_{1/2}^{0\nu 2\beta} = 2.2 \times 10^{25}$  yr has been mentioned in [13], and new experiments are in preparation both on  $^{76}\text{Ge}$  [14, 15] and other isotopes.

A more modest sensitivity was reached in the experiments searching for  $2\beta$  processes with decreasing charge of nuclei: capture of two electrons from atomic shells ( $2\varepsilon$ ), electron capture with positron emission ( $\varepsilon\beta^+$ ), and double positron decay ( $2\beta^+$ ). There are 34 possible candidates for  $2\varepsilon$  capture; among them, only 22 and 6 nuclei can also decay through  $\varepsilon\beta^+$  and  $2\beta^+$  channels, respectively [9]. In contrast to the  $2\beta^-$  decay, even the allowed  $2\nu$  mode of  $2\varepsilon$ ,  $\varepsilon\beta^+$ , and  $2\beta^+$  processes are still not detected in direct experiments|| and the obtained half-life limits are much more modest. The most

§ Massless or light bosons that arise due to a global breakdown of  $(B - L)$  symmetry, where  $B$  and  $L$  are the baryon and the lepton number, respectively. Literature considers  $0\nu 2\beta$  decay channels with one ( $0\nu 2\beta M1$ ) [4, 5], two ( $0\nu 2\beta M2$ ) [6, 7], and "bulk" ( $0\nu 2\beta bM$ ) [8] majoron emissions.

|| For completeness, we remind that a possible evidence of  $2\nu 2\varepsilon$  capture in  $^{130}\text{Ba}$  with  $T_{1/2}^{2\nu 2\varepsilon} \approx$

sensitive experiments have given limits on the  $2\varepsilon$ ,  $\varepsilon\beta^+$ , and  $2\beta^+$  processes at the level of  $10^{18} - 10^{21}$  yr [9, 11]. Reasons for such a situation are: 1) lower energy releases ( $Q_{\beta\beta}$ ) in comparison with those in  $2\beta^-$  decay, that results in lower probabilities of the processes¶, as well as provides difficulties to suppress background; 2) usually lower natural abundances ( $\delta$ ) of  $2\beta^+$  isotopes (which are typically lower than 5% with only a few exceptions<sup>+</sup>). Nevertheless, studies of  $2\varepsilon$  and  $\varepsilon\beta^+$  decays are important, because observation of neutrinoless mode of such process could help to distinguish between the mechanisms of neutrinoless  $2\beta$  decay (is it due to non-zero neutrino mass or to the right-handed admixtures in weak interactions) [18].

Zinc tungstate ( $\text{ZnWO}_4$ ) scintillators contain four potentially  $2\beta$  active isotopes:  $^{64}\text{Zn}$ ,  $^{70}\text{Zn}$ ,  $^{180}\text{W}$ , and  $^{186}\text{W}$  (see Table 1). It is worth to mention,  $^{64}\text{Zn}$  and  $^{186}\text{W}$  have comparatively large natural abundance that allows to apply  $\text{ZnWO}_4$  detectors without high cost enriched isotopes. Moreover, the  $2\nu 2\beta^-$  decay of  $^{186}\text{W}$  is expected to be strongly suppressed [19], that could provide favorable conditions to search for neutrinoless  $2\beta^-$  decays, including processes with emission of majoron(s) which have broad energy spectra, somewhat similar to that of the two neutrino mode. The  $^{180}\text{W}$  isotope is also an interesting  $2\beta$  nuclide because, in case of the capture of two electrons from the  $K$  shell ( $E_K = 65.4$  keV), the decay energy is rather small ( $13 \pm 4$ ) keV. Such a coincidence could give a resonant enhancement of the  $0\nu$  double electron capture to the corresponding level of the daughter nucleus [20, 21, 22, 23, 24, 24, 25].

**Table 1.** Potentially  $2\beta$  active isotopes of zinc and tungsten present in  $\text{ZnWO}_4$  crystal scintillators.

Transition	Energy release ( $Q_{\beta\beta}$ ), keV [26]	Isotopic abundance (%) [27]	Decay channels	Number of mother nuclei in 100 g of $\text{ZnWO}_4$ crystal
$^{64}\text{Zn} \rightarrow ^{64}\text{Ni}$	1095.7(0.7)	49.17(75)	$2\varepsilon, \varepsilon\beta^+$	$9.45 \times 10^{22}$
$^{70}\text{Zn} \rightarrow ^{70}\text{Ge}$	998.5(2.2)	0.61(10)	$2\beta^-$	$1.17 \times 10^{21}$
$^{180}\text{W} \rightarrow ^{180}\text{Hf}$	144(4)	0.12(1)	$2\varepsilon$	$2.31 \times 10^{20}$
$^{186}\text{W} \rightarrow ^{186}\text{Os}$	489.9(1.4)	28.43(19)	$2\beta^-$	$5.47 \times 10^{22}$

The best to-date half-life limits on different modes and channels of  $2\beta$  processes in zinc and tungsten isotopes (except of  $0\nu 2\beta^-$  decays of  $^{186}\text{W}$ ) were obtained in previous stages of this experiment [28, 29]. The best half-life limits on  $0\nu 2\beta^-$  decays of  $^{186}\text{W}$  to the ground and excited states of  $^{186}\text{Os}$  were set in the Solotvina experiment with cadmium tungstate scintillator enriched in  $^{116}\text{Cd}$  [30].

$(0.5 - 2.7) \times 10^{21}$  yr has been reported in geochemical studies [16, 17].

¶ The value of half-life is inversely related to the phase-space factor ( $G$ ); the latter depends on energy release as  $G \sim Q_{\beta\beta}^{11}$  for  $2\nu 2\beta$  decay and  $\sim Q_{\beta\beta}^5$  for  $0\nu 2\beta$  decay [2].

<sup>+</sup> Only 6 nuclides from a complete list of 34 isotopes-candidates on  $2\varepsilon$ ,  $\varepsilon\beta^+$ , and  $2\beta^+$  processes have natural abundances of more than 5% [9].

Here we present the final results of the experiment to search for double beta processes in zinc and tungsten with the help of  $\text{ZnWO}_4$  crystal scintillators. As a by-product of the experiment, we also have set a new limit on  $\alpha$  decay of  $^{183}\text{W}$  to the 375 keV metastable excited level of  $^{179}\text{Hf}$ .

## 2. Experiment and data analysis

The low background experiments to search for double beta processes in zinc and tungsten isotopes have been performed by using zinc tungstate crystal scintillators. The scintillation detectors with  $\text{ZnWO}_4$  crystals, the experimental set-up, the measurements and the data analysis are described in detail in [28, 29, 31]. Here we outline the main features of the experiment.

### 2.1. $\text{ZnWO}_4$ crystal scintillators

Four  $\text{ZnWO}_4$  crystal scintillators were used in our studies. Two crystals (117 g,  $20 \times 19 \times 40$  mm, and 699 g,  $\varnothing 44 \times 55$  mm) were produced by the Czochralski method [32, 33] in the Institute for Scintillation Materials (Kharkiv, Ukraine). After 2130 h of low-background measurements the crystal of 699 g was re-crystallized with the aim to study the effect of the re-crystallization on the radioactive contamination of the material. The third  $\text{ZnWO}_4$  crystal (141 g,  $\varnothing 27 \times 33$  mm, the sample had slightly irregular shape) was obtained by the re-crystallization process and used in further measurements. The fourth  $\text{ZnWO}_4$  crystal scintillator (239 g,  $\varnothing 41 \times 27$  mm) was produced in the Nikolaev Institute of Inorganic Chemistry (Novosibirsk, Russia) by the low-thermal gradient Czochralski technique [34, 35]. The radioactive contaminations of the used crystals are reported in [31].

### 2.2. Low-background measurements

The  $\text{ZnWO}_4$  crystal scintillators were fixed inside a cavity of  $\varnothing 49 \times 59$  mm in the central part of a cylindrical polystyrene light-guide of  $\varnothing 66 \times 312$  mm. The cavity was filled up with high purity silicone oil. The light-guide was optically connected on opposite sides by optical couplant to two low radioactivity EMI9265-B53/FL 3" photomultipliers (PMT). The light-guide was wrapped by PTFE reflection tape. The detector was modified at the final stages of the experiment: two polished quartz light-guides ( $\varnothing 66 \times 100$  mm) were installed between the polystyrene light-guide and the PMTs to suppress  $\gamma$  ray background from the PMTs.

The detector has been installed in the low background DAMA/R&D set-up at the underground Gran Sasso National Laboratories of the INFN (Italy) at the depth of  $\approx 3600$  m w.e. It was surrounded by Cu bricks and sealed in a low radioactive air-tight Cu box continuously flushed with high purity nitrogen gas (stored deep underground

for a long time) to avoid presence of residual environmental radon. The outer passive shield consisted of 10 cm of high purity Cu, 15 cm of low radioactive Boliden lead, 1.5 mm of cadmium and 4/10 cm polyethylene/paraffin to reduce the external background. The whole shield has been closed inside a Plexiglas box, also continuously flushed by high purity nitrogen gas. An event-by-event data acquisition system accumulates the amplitude, the arrival time, and the pulse shape of the events.

The energy scale and the energy resolution of the  $\text{ZnWO}_4$  detectors have been measured with  $\gamma$  sources  $^{22}\text{Na}$ ,  $^{60}\text{Co}$ ,  $^{133}\text{Ba}$ ,  $^{137}\text{Cs}$ ,  $^{228}\text{Th}$ , and  $^{241}\text{Am}$ . The energy resolution of the detectors (full width at half of maximum) was in the range of (8.8 – 14.6)% for 662 keV  $\gamma$  line of  $^{137}\text{Cs}$ .

### 2.3. Interpretation of the background

As an example, the energy spectrum accumulated over 4305 h with the 239 g  $\text{ZnWO}_4$  crystal scintillator in the low background set-up is shown in Fig. 1. The energy spectrum accumulated over 2798 h in the same conditions with low ( $\sim 10$  keV) energy threshold is presented in Inset. A few visible peaks in the spectrum can be ascribed to  $\gamma$  quanta of naturally occurring radionuclides  $^{40}\text{K}$ ,  $^{214}\text{Bi}$  ( $^{238}\text{U}$  chain) and  $^{208}\text{Tl}$  ( $^{232}\text{Th}$ ) from the materials of the set-up. The presence of the peak with energy  $\approx 50$  keV can be explained by internal contamination of the crystal by  $^{210}\text{Pb}$ . A comparatively wide peculiarity at the energy  $\approx 0.8$  MeV is mainly due to the  $\alpha$  active nuclides of U and Th chains present in the crystal as trace contamination.

The radiopurity of the  $\text{ZnWO}_4$  scintillators was already estimated [29, 31] by using the data of the low-background measurements. The time-amplitude analysis (see details in [36, 37]), the pulse-shape discrimination between  $\beta(\gamma)$  and  $\alpha$  particles [38], the pulse-shape analysis of the double pulses (overlapped Bi-Po events) [30, 39, 40], and the Monte Carlo simulation of the measured energy spectra were used to determine radioactive contamination of the  $\text{ZnWO}_4$  crystals. The radioactive contamination of the  $\text{ZnWO}_4$  crystals is on the level of 0.002 – 0.8 mBq/kg (depending on the source); the total  $\alpha$  activity is in the range 0.2 – 2 mBq/kg. Moreover, particular contaminations associated with the composition of  $\text{ZnWO}_4$  detector were observed [31]: the  $EC$  active cosmogenic (or/and created by neutrons) nuclide  $^{65}\text{Zn}$  ( $T_{1/2} = 244.26$  d [41]) with activity 0.5 – 0.8 mBq/kg (depending on the  $\text{ZnWO}_4$  sample) and the  $\alpha$  active tungsten isotope  $^{180}\text{W}$  (with half-life:  $T_{1/2} \approx 10^{18}$  yr [31, 39, 42, 43], and energy of the decay:  $Q_\alpha = 2508(4)$  keV [26]) with activity 0.04 mBq/kg (see Fig. 1).

## 3. Results and discussion

### 3.1. Response of the $\text{ZnWO}_4$ detectors to $2\beta$ processes in zinc and tungsten

The response functions of the  $\text{ZnWO}_4$  detectors for the  $2\beta$  processes in Zn and W isotopes were simulated with the help of the GEANT4 package [44] with the Low Energy

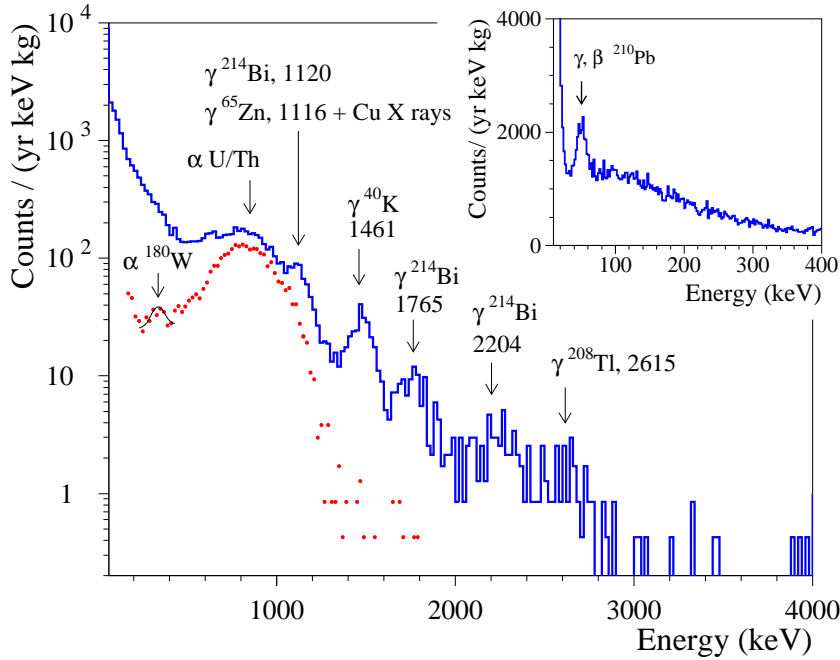


**Figure 1.** (Color online) The energy spectrum accumulated with the  $\text{ZnWO}_4$  crystal scintillator  $\varnothing 41 \times 27$  mm in the low background DAMA/R&D set-up over 4305 h. The energy spectrum of  $\alpha$  events selected by the pulse-shape discrimination is drawn by points. Fit of the  $\alpha$  peak of  $^{180}\text{W}$  by Gaussian function (solid line) is shown. (Inset) The energy spectrum of  $\gamma$  and  $\beta$  events selected by the pulse-shape discrimination technique from the data measured over 2798 h with the same crystal scintillator in the set-up with lower energy threshold and with additional quartz light-guides. Energies of  $\gamma$  lines are in keV.

Electromagnetic extensions. The initial kinematics of the particles emitted in the decays was generated with the DECAY0 event generator [45]. As examples, the expected energy distributions for the  $\text{ZnWO}_4$  detector  $\varnothing 44 \times 55$  mm are shown in Fig. 2 and Fig. 3. The background models included the internal contamination of the  $\text{ZnWO}_4$  scintillators ( $^{40}\text{K}$ ,  $^{60}\text{Co}$ ,  $^{65}\text{Zn}$ ,  $^{87}\text{Rb}$ ,  $^{90}\text{Sr}$ - $^{90}\text{Y}$ ,  $^{137}\text{Cs}$ , active nuclides from U/Th families), and the external  $\gamma$  rays from radioactive contamination of the PMTs and the copper box ( $^{40}\text{K}$ ,  $^{232}\text{Th}$ ,  $^{238}\text{U}$ ); they were also simulated with the help of the GEANT4 and DECAY0 packages.

### 3.2. Double $\beta$ processes in $^{64,70}\text{Zn}$ and $^{180,186}\text{W}$

Comparing the simulated response functions with the measured energy spectra of the  $\text{ZnWO}_4$  detectors, we have not found clear peculiarities, which can be evidently attributed to double beta decay of zinc or tungsten isotopes. Therefore only lower half-life limits can be set according to the formula:

$$\lim T_{1/2} = N \cdot \eta \cdot t \cdot \ln 2 / \lim S, \quad (1)$$

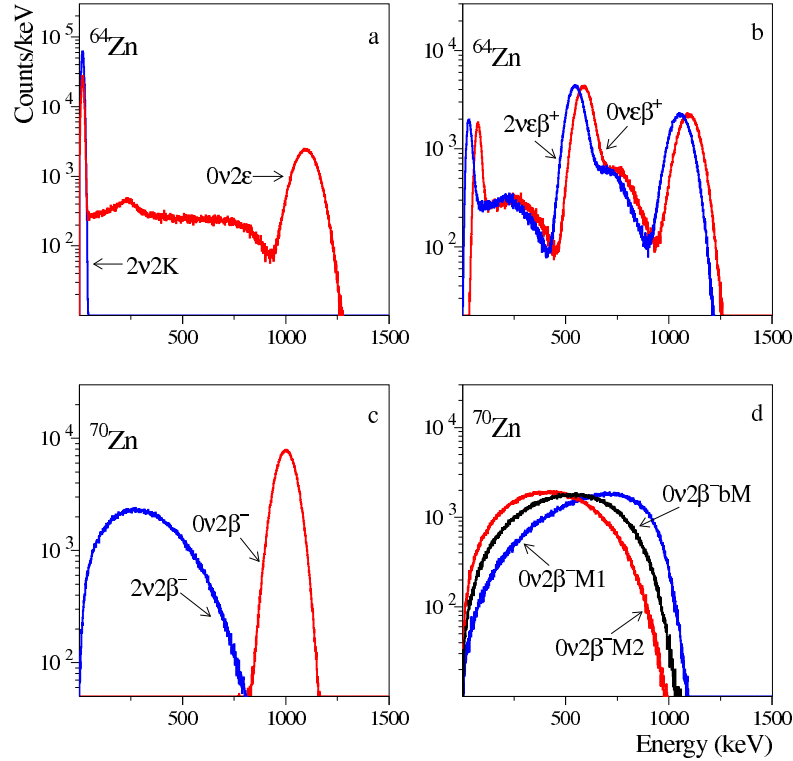


**Figure 2.** (Color online) Simulated response functions of the detector based on the  $\text{ZnWO}_4$  scintillator  $\varnothing 44 \times 55$  mm for the different  $2\beta$  processes in Zn isotopes: (a)  $2\varepsilon$  capture in  $^{64}\text{Zn}$ ; (b)  $\varepsilon\beta^+$  decay of  $^{64}\text{Zn}$ ; (c)  $2\beta^-$  decay of  $^{70}\text{Zn}$ ; (d)  $0\nu 2\beta^-$  processes with majorons emissions in  $^{70}\text{Zn}$ . One million decays was simulated for each process.

where  $N$  is the number of potentially  $2\beta$  unstable nuclei in a crystal scintillator,  $\eta$  is the detection efficiency,  $t$  is the measuring time, and  $\lim S$  is the number of events of the effect searched for which can be excluded at a given confidence level (C.L.; all the limits in the present study are given at 90% C.L.).

For the  $2\nu$  double electron capture in  $^{64}\text{Zn}$  from the  $K$  shell, the total energy released in the detector is equal to  $2E_K = 16.7$  keV (where  $E_K$  is the binding energy of electrons on the  $K$  shell of nickel atoms). The detection of such a small energy deposit requires rather low energy threshold. In our measurements with the  $\text{ZnWO}_4$  crystal scintillator  $\varnothing 41 \times 27$  mm the energy threshold of 10 keV was enough low (see Fig. 1, Inset) to observe at least the higher energy part of the  $2\nu 2K$  peak. Moreover, the background level (which is mainly due to PMT noise in the low energy region) was decreased in comparison to our first measurement [28] thanks to the improved scintillation properties of the  $\text{ZnWO}_4$  crystal (slightly higher transmittance, light output and energy resolution) and the enhanced light collection from the scintillator. The light collection was increased by special treatment of the crystal surface, which was diffused with the help of grinding paper (in our first experiment, the  $\text{ZnWO}_4$  crystal scintillator was polished [28]). Finally, a significant difference of  $\text{ZnWO}_4$  pulse-shape (effective decay time is  $\approx 24 \mu\text{s}$  [46]) in comparison to much faster PMT noise (few nanoseconds) offers the possibility to exploit

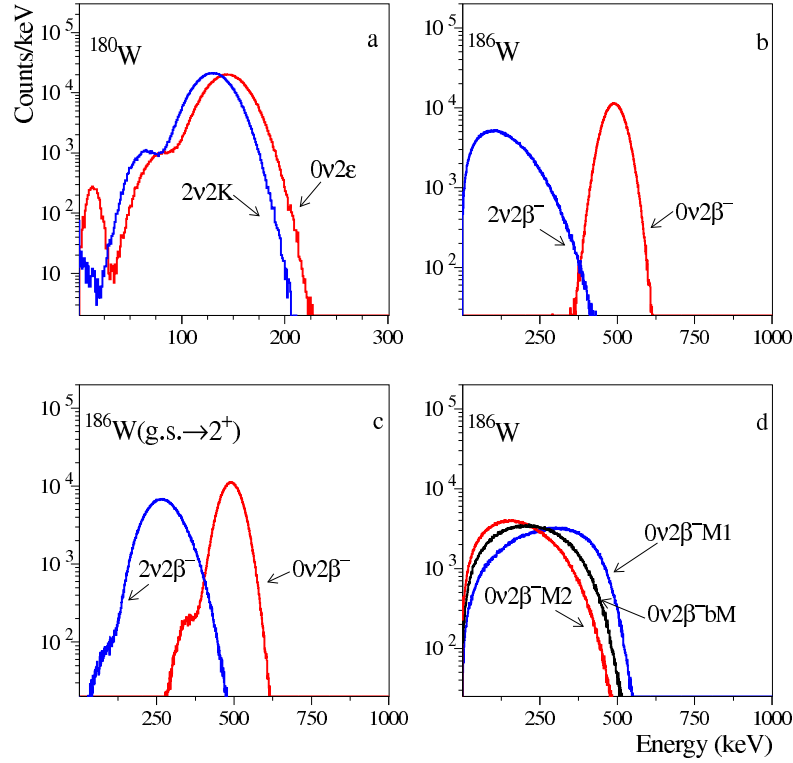


**Figure 3.** (Color online) Simulated response functions of the  $\text{ZnWO}_4$  detector  $\varnothing 44 \times 55$  mm for the different  $2\beta$  processes in W isotopes: (a)  $2\epsilon$  capture in  $^{180}\text{W}$ ; (b) and (c)  $2\beta^-$  decay of  $^{186}\text{W}$  to the ground and excited states of  $^{186}\text{Os}$ , respectively; (d)  $0\nu 2\beta^-$  decays of  $^{186}\text{W}$  with majorons emissions. One million decays was simulated for each process.

the rejection of residual PMT noise by using the pulse-shape discrimination. However, this procedure eliminates some part of scintillation signals near energy threshold. The energy dependence of the detection efficiency was determined with the help of  $^{133}\text{Ba}$ ,  $^{137}\text{Cs}$ ,  $^{228}\text{Th}$ , and  $^{241}\text{Am}$  radioactive sources. The measured efficiency ranges from about 55% at 15 keV up to about 95% at 30 keV (one can compare these values with the detection efficiencies 30% at 15 keV and 65% at 30 keV obtained in [28]).

To set a limit on the  $2\nu 2K$  decay of  $^{64}\text{Zn}$ , taking into account the proximity of the energy threshold and the contribution from remaining PMT noise, we use a conservative requirement: the theoretical energy distribution should not exceed the experimental one in any energy interval, including error bars in the experimental values (see Fig. 4). In this way the limit on the peak area is  $\lim S = 4665$  counts. Taking this value (already corrected for the efficiency) for the peak area, we conservatively give the following half-life limit on the  $2\nu 2K$  process:

$$T_{1/2}^{2\nu 2K}(^{64}\text{Zn}) \geq 1.1 \times 10^{19} \text{ yr.}$$

To estimate limits on other double  $\beta$  processes, we have used the following approach: the energy spectrum was fitted in the energy range of an expected  $2\beta$  signal by a model

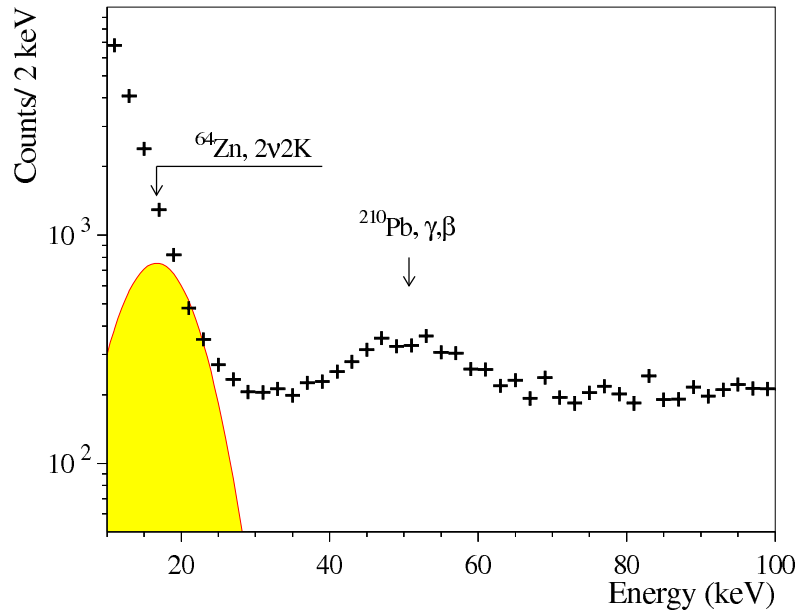


**Figure 4.** The energy spectrum of the  $\text{ZnWO}_4$  crystal scintillator  $\varnothing 41 \times 27$  mm measured over 2798 h, corrected for the energy dependence of detection efficiency, together with the  $2\nu 2K$  peak of  $^{64}\text{Zn}$  with  $T_{1/2}^{2\nu 2K} = 1.1 \times 10^{19}$  yr excluded at 90% C.L.

built by the simulated distributions of internal and external background and of the effect searched for. The background model was composed of  $^{40}\text{K}$ ,  $^{65}\text{Zn}$ ,  $^{90}\text{Sr}$ - $^{90}\text{Y}$ ,  $^{137}\text{Cs}$ , U/Th inside a crystal (for fit of a low energy part of the data we have also used a model of internal  $^{87}\text{Rb}$ ), and  $^{40}\text{K}$ ,  $^{232}\text{Th}$ ,  $^{238}\text{U}$  in the PMTs and the copper box. The activities of the U/Th daughters in the crystals have been restricted taking into account the data on the radioactive contamination of the  $\text{ZnWO}_4$  crystal scintillators [31]. The initial values of the  $^{40}\text{K}$ ,  $^{232}\text{Th}$  and  $^{238}\text{U}$  activities inside the PMTs have been taken from Ref. [47], while activities inside the copper box have been assumed to be equal to the estimations obtained in Ref. [48]. We have used different combinations of the accumulated data to reach the maximal sensitivity to the double beta processes searched for. Additionally we have also applied the so called  $1\sigma$  approach when a statistical uncertainty of the number of events accumulated in the energy region of the expected  $2\beta$  signal (square root of the number of events) was taken as  $\text{lim } S$ . This simple method allows to obtain a correct evaluation of the experimental sensitivity to the  $2\beta$  process searched for. It should be stressed that the detection efficiencies in all the distributions analyzed are at least 99.9% for all the processes. Taking into account the efficiency of  $\gamma(\beta)$  events selection by the pulse-shape discrimination (98%), the total detection efficiencies are at least 97.9% for all the  $2\beta$  processes searched for.

Let us give an example of the analysis by using the two approaches to search for electron capture with positron emission in  $^{64}\text{Zn}$ . 14922 events were observed in the energy interval 530 – 1190 keV of the spectrum accumulated with an exposure 0.3487 kg  $\times$  yr (see Fig. 5), which gives  $\text{lim } S = 122$  counts. With the detection efficiency

in the energy interval to the  $2\nu\varepsilon\beta^+$  decay of  $^{64}\text{Zn}$  (82%), one obtains the half-life limit  $T_{1/2}^{2\nu\varepsilon\beta^+} \geq 1.5 \times 10^{21}$  yr at 68% C.L. In order to apply the second approach, the starting and final energies of the fit were varied as 380–550 keV and 1260–1430 keV, respectively, with the step of 10 keV. The result of the fit in the energy region 520 – 1350 keV was chosen as final giving the minimal value of  $\chi^2/n.d.f. = 119/98 = 1.23$ . It gives the total area of the  $2\nu\varepsilon\beta^+$  effect ( $-208 \pm 254$ ) counts which corresponds (in accordance with the Feldman-Cousins procedure [49]) to  $\text{lim } S = 238$  counts in the full energy distributions for  $2\nu\varepsilon\beta^+$  decay. Thus, one can calculate the following half-life limit, rather similar to the value obtained by using the  $1\sigma$  approach:

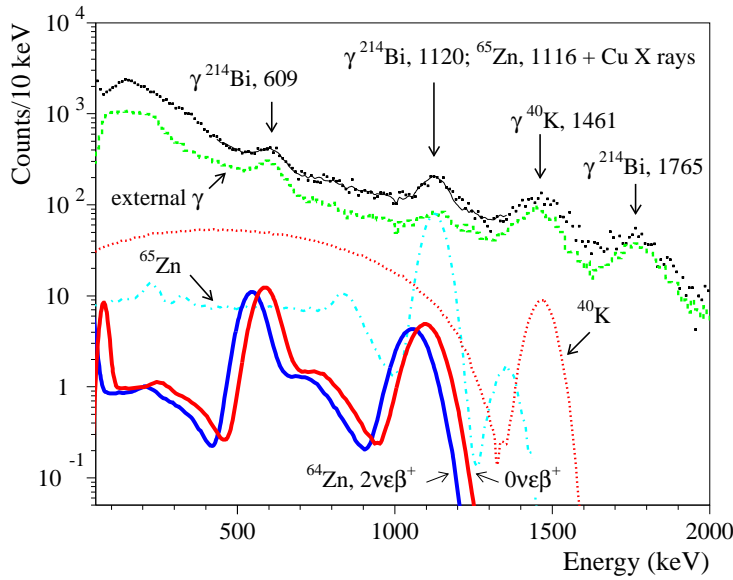


**Figure 5.** (Color online) The measured energy spectrum of the  $\text{ZnWO}_4$  scintillation crystals (the total exposure is  $0.349 \text{ kg} \times \text{yr}$ ) together with the GEANT4-simulated response functions for  $\varepsilon\beta^+$  process in  $^{64}\text{Zn}$  excluded at 90% C.L. The most important components of the background are shown. The energies of  $\gamma$  lines are in keV.

$$T_{1/2}^{2\nu\varepsilon\beta^+} (^{64}\text{Zn}) \geq 9.4 \times 10^{20} \text{ yr.}$$

In case of the neutrinoless electron capture with positron emission, the spectrum with the total exposure  $0.3487 \text{ kg} \times \text{yr}$  was fitted in the energy interval (410 – 1370) keV ( $\chi^2/n.d.f. = 113/94 = 1.2$ ). The fit gives the area of the effect searched for as  $(52 \pm 129)$  counts, which corresponds (again in accordance with the Feldman-Cousins procedure) to  $\text{lim } S = 264$  events. It allows to set the following limit on the half-life of  $^{64}\text{Zn}$  relatively to the  $0\nu\varepsilon\beta^+$  decay:

$$T_{1/2}^{0\nu\varepsilon\beta^+} (^{64}\text{Zn}) \geq 8.5 \times 10^{20} \text{ yr.}$$

The energy distributions expected for the  $2\nu\varepsilon\beta^+$  and  $0\nu\varepsilon\beta^+$  decay of  $^{64}\text{Zn}$ , excluded at 90% C.L., are shown in Fig. 5.

In case of  $0\nu 2\varepsilon$  decay of  $^{64}\text{Zn}$ , different particles are emitted: X rays and Auger electrons from deexcitations in atomic shells,  $\gamma$  quanta and/or conversion electrons from deexcitation of daughter nucleus. We suppose here that only one  $\gamma$  quantum is emitted in the nuclear deexcitation process; it is the most pessimistic scenario from the point of view of registration of such an event in a peak of full absorption at the  $Q_{\beta\beta}$  energy. Unfortunately,  $2K$ ,  $KL$ ,  $2L$  (and other) modes are not energetically resolved in the high energy region due to finite energy resolution of the  $\text{ZnWO}_4$  detectors. So, the fit of the measured spectrum (exposure  $0.3647 \text{ kg} \times \text{yr}$ ) in the energy interval  $440 - 1350 \text{ keV}$  ( $\chi^2/n.d.f. = 98/89 = 1.1$ ) gives the area of the  $0\nu 2\varepsilon$  effect searched for as  $(-780 \pm 853)$  counts. Taking into account the Feldman-Cousins procedure, we calculated  $\text{lim } S = 742$  events and the following limit on  $0\nu 2\varepsilon$  transition of  $^{64}\text{Zn}$  to ground state of  $^{64}\text{Ni}$ :

$$T_{1/2}^{0\nu 2\varepsilon}(^{64}\text{Zn}) \geq 3.2 \times 10^{20} \text{ yr.}$$

Limits on double electron capture in  $^{180}\text{W}$  were set by analyzing all the data accumulated in the experiment over  $0.529 \text{ kg} \times \text{yr}$ . The low energy part of the spectrum is shown in Fig. 6. The least squares fit of this spectrum in the  $100 - 260 \text{ keV}$  energy interval gives  $(141 \pm 430)$  counts for the  $2\nu 2K$  peak searched for ( $\chi^2/n.d.f. = 5.39/5 = 1.08$ ), providing no evidence for the effect. These numbers lead to an upper limit of 846 counts. Taking into account the detection efficiency for this process close to 98%, one can calculate the half-life limit:

$$T_{1/2}^{2\nu 2K}(^{180}\text{W}) \geq 1.0 \times 10^{18} \text{ yr.}$$

The same approach gives the limit for the neutrinoless  $2\varepsilon$  process in  $^{180}\text{W}$ :

$$T_{1/2}^{0\nu 2\varepsilon}(^{180}\text{W}) \geq 1.3 \times 10^{18} \text{ yr.}$$

The expected energy distributions for  $0\nu 2\varepsilon$  and  $2\nu 2K$  decay of  $^{180}\text{W}$  corresponding to the best previous restrictions obtained in the Solotvina experiment [30] with the help of low background cadmium tungstate crystal scintillators are presented in Fig. 6. Advancement of the sensitivity in the present study was reached thanks to the lower background of  $\text{ZnWO}_4$  detectors in comparison to  $\text{CdWO}_4$  where the counting rate in the energy interval up to  $0.4 \text{ MeV}$  was caused mainly by the  $\beta$  decay of  $^{113}\text{Cd}$ . The  $0\nu 2\varepsilon$  decay of  $^{180}\text{W}$  is of particular interest due to the possibility of resonant process [23, 24, 25].

By using the approaches described above, the half-life limits on other  $2\beta$  decay processes in  $^{64}\text{Zn}$ ,  $^{70}\text{Zn}$ , and  $^{186}\text{W}$  have been obtained. All the results are summarized in Table 2, where the data of the most sensitive previous experimental investigations and theoretical estimations are given for comparison.

The obtained bounds are well below the existing theoretical predictions; nevertheless most of the limits are higher than those established in previous experiments. It should be stressed that in contrast to the results obtained in researches of double  $\beta^-$  decay (sensitivity of the best experiments is on the level of  $10^{23} - 10^{25} \text{ yr}$  [9, 10, 11]), only five nuclides ( $^{40}\text{Ca}$  [50],  $^{64}\text{Zn}$  [present work],  $^{78}\text{Kr}$  [51],  $^{112}\text{Sn}$  [52], and  $^{120}\text{Te}$  [53])

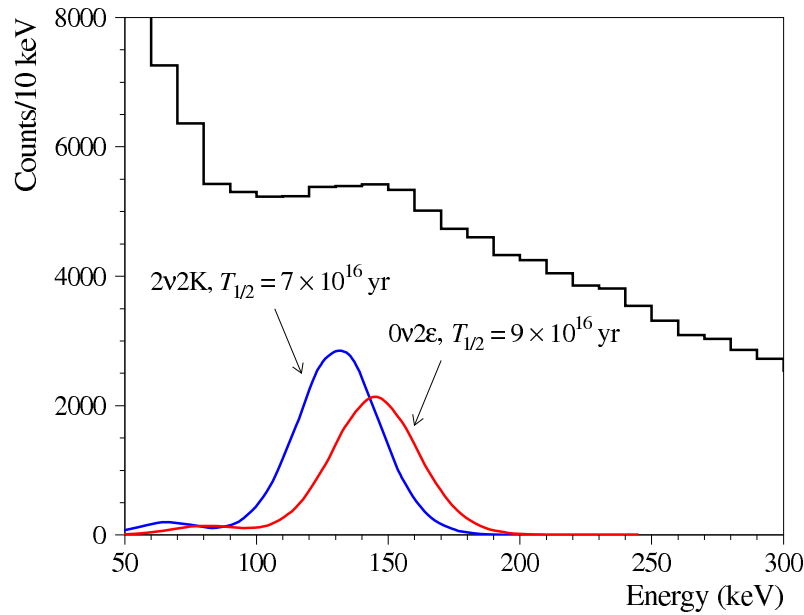


**Figure 6.** (Color online) Energy spectrum of the background of the  $\text{ZnWO}_4$  detectors (exposure  $0.529 \text{ kg} \times \text{yr}$ ). The simulated response functions for double electron capture in  $^{180}\text{W}$  are shown; the half-lives  $T_{1/2}^{2\nu 2K} = 7 \times 10^{16} \text{ yr}$  and  $T_{1/2}^{0\nu 2\varepsilon} = 9 \times 10^{16} \text{ yr}$  correspond to the best previous limits obtained in [30] with the help of cadmium tungstate crystal scintillators.

among 34 potentially  $2\varepsilon$ ,  $\varepsilon\beta^+$ , and  $2\beta^+$  active isotopes were investigated at the level of sensitivity  $\text{lim } T_{1/2} \sim 10^{21} \text{ yr}$ .

### 3.3. Search for $\alpha$ decay of tungsten isotopes

In addition to the previous observation of the  $\alpha$  decay  $^{180}\text{W} \rightarrow ^{176}\text{Hf}$  (g.s. to g.s. transition) with  $\text{CdWO}_4$  and  $\text{CaWO}_4$  detectors [39, 42, 43], this rare process was observed also in our data with  $\text{ZnWO}_4$  scintillators with  $T_{1/2} = 1.3_{-0.5}^{+0.6} \times 10^{18} \text{ yr}$  [31] (one can also see the  $\alpha$  peak of  $^{180}\text{W}$  in the  $\alpha$  spectrum presented in Fig. 1).

Here we report a new limit on the  $\alpha$  decay of  $^{183}\text{W}$  ( $Q_\alpha = 1680(2) \text{ keV}$  [26];  $\delta = 14.31(4)\%$  [27]) to the  $1/2^-$  metastable level of  $^{179}\text{Hf}$  (375 keV,  $T_{1/2} = 18.67 \text{ s}$  [41]). The search for this process has been performed by using the data of all the runs with the  $\text{ZnWO}_4$  detectors with the total exposure  $0.5295 \text{ kg} \times \text{yr}$ . The signature of such a transition is delayed  $\gamma$  quanta after the emission of the  $\alpha$  particle. The expected distribution of the time intervals between the  $\alpha$  and the  $\gamma$  events should correspond to  $T_{1/2} = 18.67 \text{ s}$ . The time-amplitude technique [36, 37] and the pulse-shape discrimination method [38, 46] have been applied to search for the  $\alpha$  decay. Taking into account the  $\alpha/\beta$  ratio\* ( $\alpha/\beta \approx 0.17$ ) for the  $\text{ZnWO}_4$  scintillator [46], we expect to observe the  $\alpha$  peak of the  $^{183}\text{W}$  decay to the  $^{179}\text{Hf}$  metastable level at the energy 220 keV in  $\gamma$  scale,

\* It is defined as ratio of  $\alpha$  peak position in the energy scale measured with  $\gamma$  sources to the real energy of  $\alpha$  particles.

**Table 2.** Half-life limits on  $2\beta$  processes in Zn and W isotopes and comparison with the theoretical predictions. Quoting best previous experimental results, we exclude limits obtained on previous stages of our experiment [28, 29].

Transition	Decay channel	Level of daughter nucleus	Experimental limits on $T_{1/2}$ , yr at 90% C.L.		Theoretical estimations of the half-lives $T_{1/2}$ , yr ( $\langle m_\nu \rangle = 1$ eV for $0\nu 2\beta$ decay)
			Present work	The best previous results	
$^{64}\text{Zn} \rightarrow ^{64}\text{Ni}$	$2\nu 2K$	g.s.	$\geq 1.1 \times 10^{19}$	$\geq 6.0 \times 10^{16}$ [54]	$(1.9 - 7.1) \times 10^{26}$ [56] $(1.2 \pm 0.2) \times 10^{25}$ [57]
	$0\nu 2\varepsilon$	g.s.	$\geq 3.2 \times 10^{20}$	$\geq 7.4 \times 10^{18}$ [55]	–
	$2\nu \varepsilon \beta^+$	g.s.	$\geq 9.4 \times 10^{20}$	$= (1.1 \pm 0.9) \times 10^{19}$ [58] $\geq 1.3 \times 10^{20}$ [59]	$(0.9 - 2.2) \times 10^{35}$ [56] $(4.7 \pm 0.9) \times 10^{31}$ [57]
	$0\nu \varepsilon \beta^+$	g.s.	$\geq 8.5 \times 10^{20}$	$\geq 1.3 \times 10^{20}$ [59]	–
$^{70}\text{Zn} \rightarrow ^{70}\text{Ge}$	$2\nu 2\beta^-$	g.s.	$\geq 3.8 \times 10^{18}$	$\geq 1.3 \times 10^{16}$ [46]	$4.5 \times 10^{21} - 3.6 \times 10^{24}$ [60] $2.5 \times 10^{21} - 6.4 \times 10^{23}$ [61] $7.0 \times 10^{23}$ [56] $\geq 3.1 \times 10^{22}$ [62] $9.8 \times 10^{25}$ [60]
	$0\nu 2\beta^-$	g.s.	$\geq 3.2 \times 10^{19}$	$\geq 7.0 \times 10^{17}$ [46]	–
	$0\nu 2\beta^- M1$	g.s.	$\geq 6.0 \times 10^{18}$	–	–
	$0\nu 2\beta^- M2$	g.s.	$\geq 4.7 \times 10^{18}$	–	–
	$0\nu 2\beta^- bM$	g.s.	$\geq 5.4 \times 10^{18}$	–	–
$^{180}\text{W} \rightarrow ^{180}\text{Hf}$	$2\nu 2K$	g.s.	$\geq 1.0 \times 10^{18}$	$\geq 7.0 \times 10^{16}$ [30]	–
	$0\nu 2\varepsilon$	g.s.	$\geq 1.3 \times 10^{18}$	$\geq 9.0 \times 10^{16}$ [30]	$2.5 \times 10^{24} - 2.5 \times 10^{26}$ [23] $3.3 \times 10^{27} - 5.0 \times 10^{30}$ [24] $3.0 \times 10^{22} - 4.0 \times 10^{27}$ [25]
$^{186}\text{W} \rightarrow ^{186}\text{Os}$	$2\nu 2\beta^-$	g.s.	$\geq 2.3 \times 10^{19}$	$\geq 3.7 \times 10^{18}$ [30]	$7.1 \times 10^{23} - 1.2 \times 10^{25}$ [60] $\geq 6.1 \times 10^{24}$ [19]
	$2\nu 2\beta^-$	$2_1^+$ (137 keV)	$\geq 1.8 \times 10^{20}$	$\geq 1.0 \times 10^{19}$ [30]	–
	$0\nu 2\beta^-$	g.s.	$\geq 1.0 \times 10^{21}$	$\geq 1.1 \times 10^{21}$ [30]	$6.4 \times 10^{24}$ [60]
	$0\nu 2\beta^-$	$2_1^+$ (137 keV)	$\geq 9.0 \times 10^{20}$	$\geq 1.1 \times 10^{21}$ [30]	–
	$0\nu 2\beta^- M1$	g.s.	$\geq 5.8 \times 10^{19}$	$\geq 1.2 \times 10^{20}$ [30]	–
	$0\nu 2\beta^- M2$	g.s.	$\geq 1.1 \times 10^{19}$	–	–
	$0\nu 2\beta^- bM$	g.s.	$\geq 1.1 \times 10^{19}$	–	–

with energy resolution  $\text{FWHM}_\alpha = 62$  keV. All the  $\alpha$  events selected within 150–270 keV have been used as triggers, while a time interval 0.1 – 60 s (88.9% of  $^{179}\text{Hf}^*$  decays) and a 325 – 425 keV energy window have been set for the second  $\gamma$  events (energy resolution for gammas at the energy 375 keV:  $\text{FWHM}_\gamma = 64$  keV). Ninety five pairs were selected from the data. The fit of the distribution of the selected “ $\alpha$  events” by a simple model built by a first degree polynomial function (to describe the background) plus a Gaussian (the  $\alpha$  peak searched for) gives the area of the effect searched for as  $(10.5 \pm 17.6)$  counts, which corresponds to  $\text{lim } S = 39.4$  events. The excited 375 keV level of  $^{179}\text{Hf}$  deexcites with emission of two  $\gamma$  quanta of 161 keV and 214 keV [41]. The efficiency to detect a peak at the total energy release of 375 keV in  $\text{ZnWO}_4$  detectors was calculated with the GEANT4 [44]; it was equal 0.71 to 0.86 in dependence on the volume of the  $\text{ZnWO}_4$  crystal. The half-life limit was calculated according to the formula analogous to (1):

$$\text{lim } T_{1/2} = \ln 2 \cdot \eta_{PSD} \cdot \sum \eta \cdot N \cdot t / \text{lim } S,$$

where  $\eta_{PSD}$  is the efficiency of the pulse-shape discrimination (37.2%),  $N$  is the number of  $^{183}\text{W}$  nuclei,  $\eta$  is the registration efficiency of the total energy release of 375 keV, and  $t$  is the time of measurements with specific  $\text{ZnWO}_4$  detector. In result, we set the

following limit on the half-life of the  $\alpha$  decay of  $^{183}\text{W}$  to the metastable 375 keV excited level of  $^{179}\text{Hf}$ :

$$T_{1/2}^{\alpha} (^{183}\text{W} \rightarrow ^{179}\text{Hf}^*, 375 \text{ keV}) \geq 6.7 \times 10^{20} \text{ yr.}$$

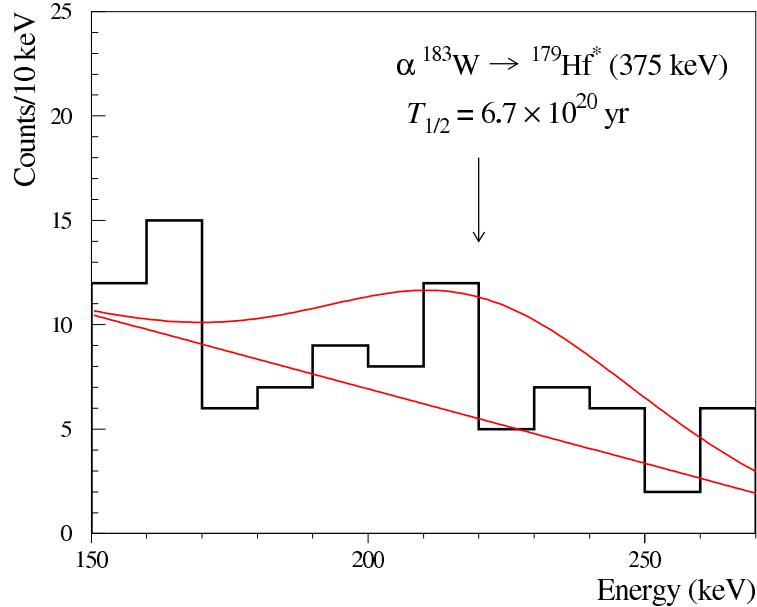


**Figure 7.** (Color online) Energy spectrum of the events selected by the time-amplitude and the pulse-shape analyses from the data accumulated by  $\text{ZnWO}_4$  detectors with an exposure  $0.5295 \text{ kg} \times \text{yr}$ . These events satisfy the search criteria for  $\alpha$  transition of  $^{183}\text{W}$  to metastable level of  $^{179}\text{Hf}$ . Polynomial function used as a background model and the Gaussian peak corresponding to  $\alpha$  decay of  $^{183}\text{W}$  with the half-life  $T_{1/2} = 6.7 \times 10^{20} \text{ yr}$  excluded at 90% C.L. are also shown.

The energy spectrum of the selected events is shown in Fig. 7 together with the excluded  $\alpha$  peak of  $^{183}\text{W}$ .

Despite the obtained limit is far away from the theoretical predictions (f.i.,  $T_{1/2} \approx 1.3 \times 10^{50} \text{ yr}$  [63]), the limit is almost two orders higher than the previous one  $T_{1/2} \geq 1.0 \times 10^{19} \text{ yr}$  derived from the low background measurements with a small (4.5 g)  $\text{ZnWO}_4$  crystal scintillator [64].

#### 4. Conclusions

A low background experiment to search for  $2\beta$  processes in  $^{64}\text{Zn}$ ,  $^{70}\text{Zn}$ ,  $^{180}\text{W}$ , and  $^{186}\text{W}$  was carried out over more than 19 thousands hours in the underground Gran Sasso National Laboratories of the INFN by using radiopure  $\text{ZnWO}_4$  crystal scintillators. The total exposure of the experiment is  $0.5295 \text{ kg} \times \text{yr}$ .

New improved half-life limits on double electron capture and electron capture with positron emission in  $^{64}\text{Zn}$  have been set in the range:  $10^{19} \text{ yr}$  to  $10^{21} \text{ yr}$  depending on the mode. The indication on the  $(2\nu + 0\nu)\epsilon\beta^+$  decay of  $^{64}\text{Zn}$  with  $T_{1/2} = (1.1 \pm 0.9) \times 10^{19} \text{ yr}$

suggested in [58] is completely disproved by the results of the present experiment. Note that to date only four nuclides ( $^{40}\text{Ca}$ ,  $^{78}\text{Kr}$ ,  $^{112}\text{Sn}$ , and  $^{120}\text{Te}$ ) among 34 candidates to  $2\varepsilon$ ,  $\varepsilon\beta^+$ , and  $2\beta^+$  processes were studied at similar level of sensitivity in direct experiments. However, it is worth noting that the limits are still far from theoretical predictions.

In addition to  $^{64}\text{Zn}$  decays, in the course of the present experiment two important by-products were obtained: (1) the new half-life limits on the  $2\beta$  processes in  $^{70}\text{Zn}$ ,  $^{180}\text{W}$ , and  $^{186}\text{W}$  on the level of  $10^{18} - 10^{21}$  yr (the  $0\nu 2\varepsilon$  capture in  $^{180}\text{W}$  is of particular interest due to the possibility of resonant process); (2) rare  $\alpha$  decay of  $^{180}\text{W}$  with a half-life  $T_{1/2} = 1.3_{-0.5}^{+0.6} \times 10^{18}$  yr has been observed and new half-life limit on  $\alpha$  transition of  $^{183}\text{W}$  to the  $1/2^-$  375 keV metastable level of  $^{179}\text{Hf}$  has been set as  $T_{1/2} \geq 6.7 \times 10^{20}$  yr.

## 5. Acknowledgments

The group from the Institute for Nuclear Research (Kyiv, Ukraine) was supported in part by the Project "Kosmomikrofizyka-2" (Astroparticle Physics) of the National Academy of Sciences of Ukraine. D.V. Poda was also partly supported by the Project "Double beta decay and neutrino properties" for young scientists of the National Academy of Sciences of Ukraine (Reg. No. 0110U004150).

## References

- [1] W. Rodejohann, Neutrino-less double beta decay and particle physics, arXiv:1106.1334 [hep-ph], submitted to Int. J. Mod. Phys. E;  
F.T. Avignone III, S.R. Elliott, and J. Engel, Rev. Mod. Phys. 80 (2008) 481;  
H.V. Klapdor-Kleingrothaus, Int. J. Mod. Phys. E 17 (2008) 505.
- [2] H. Ejiri, J. Phys. Soc. Japan 74 (2005) 2101;  
F.T. Avignone III, G.S. King, and Yu.G. Zdesenko, New J. Phys. 7 (2005) 6;  
S.R. Elliot and J. Engel, J. Phys. G: Nucl. Part. Phys. 30 (2004) R183;  
J.D. Vergados, Phys. Rep. 361 (2002) 1;  
S.R. Elliot and P. Vogel, Ann. Rev. Nucl. Part. Sci. 52 (2002) 115;  
Yu.G. Zdesenko, Rev. Mod. Phys. 74 (2002) 663.
- [3] U. Dore and D. Orestano, Rep. Prog. Phys. 71 (2008) 106201;  
R.N. Mohapatra et al., Rep. Prog. Phys. 70 (2007) 1757.
- [4] R.N. Mohapatra and P.B. Pal, *Massive Neutrinos in Physics and Astrophysics*, 3rd ed., World Sci., 2004.
- [5] Z.G. Berezhiani, A.Yu. Smirnov, and J.W.F. Valle, Phys. Lett. B 219 (1992) 99.
- [6] R.N. Mohapatra and E. Takasugi, Phys. Lett. B 211 (1988) 192.
- [7] P. Bamert, C.P. Burgess, and R.N. Mohapatra, Nucl. Phys. B 449 (1995) 25.
- [8] R.N. Mohapatra, A. Perenz-Lorenzana, and C.A. de Pires, Phys. Lett. B 491 (2000) 143.
- [9] V.I. Tretyak and Yu.G. Zdesenko, At. Data Nucl. Data Tables 61 (1995) 43; 80 (2002) 83.
- [10] A.S. Barabash, Phys. Rev. C 81 (2010) 035501.
- [11] A.S. Barabash, Phys. At. Nucl. 73 (2010) 162.
- [12] N. Ackerman et al., arXiv:1108.4193v1 [nucl-ex].
- [13] H.V. Klapdor-Kleingrothaus and I.V. Krivosheina, Mod. Phys. Lett. A 21 (2006) 1547.
- [14] I. Abt et al., hep-ex/0404039;  
A.A. Smolnikov and GERDA Collab., nucl-ex/0812.4194.

- [15] Majorana Collab., nucl-ex/0311013;  
C.E. Aalseth et al., Nucl. Phys. B (Proc. Suppl.) 138 (2005) 217.
- [16] A.P. Meshik, C.M. Hohenberg, O.V. Pravdivtseva, and Ya.S. Kapusta, Phys. Rev. C 64 (2001) 035205.
- [17] M. Pujol, B. Marty, P. Burnard, and P. Philippot, Geochim. Cosmochim. Acta 73 (2009) 6834.
- [18] M. Hirsch et al., Z. Phys. A 347 (1994) 151.
- [19] O. Castanos, J.G. Hirsch, O. Civitarese, and P.O. Hess, Nucl. Phys. A 571 (1994) 276.
- [20] R.G. Winter, Phys. Rev. 100 (1955) 142.
- [21] M.B. Voloshin, G.V. Mitsel'makher, and R.A. Eramzhyan, JETP Lett. 35 (1982) 656.
- [22] J. Bernabeu et al., Nucl. Phys. B 223 (1983) 15.
- [23] Z. Sujkowski and S. Wycech, Acta Phys. Pol. B 33 (2002) 471.
- [24] Z. Sujkowski and S. Wycech, Phys. Rev. C 70 (2004) 052501.
- [25] M.I. Krivoruchenko, F. Šimkovic, D. Frekers, and A. Faessler, Nucl. Phys. A 859 (2011) 140.
- [26] G. Audi, O. Bersillon, J. Blachot, and A.H. Wapstra, Nucl. Phys. A 729 (2003) 337.
- [27] M. Berglund and M.E. Wieser, Pure Appl. Chem. 83 (2011) 397.
- [28] P. Belli et al., Phys. Lett. B 658 (2008) 193.
- [29] P. Belli et al., Nucl. Phys. A 826 (2009) 256.
- [30] F.A. Danevich et al., Phys. Rev. C 68 (2003) 035501.
- [31] P. Belli et al., Nucl. Instr. Meth. A 626-627 (2010) 31.
- [32] L.L. Nagornaya et al., IEEE Trans. Nucl. Sci. 55 (2008) 1469.
- [33] L.L. Nagornaya et al., IEEE Trans. Nucl. Sci. 56 (2009) 2513.
- [34] E.N. Galashov, V.A. Gusev, V.N. Shlegel, and Ya.V. Vasiliev, Func. Mat. 16 (2009) 63.
- [35] E.N. Galashov et al., Crystallogr. Rep. 54 (2009) 689.
- [36] F.A. Danevich et al., Phys. Lett. B 344 (1995) 72.
- [37] F.A. Danevich et al., Nucl. Phys. A 694 (2001) 375.
- [38] E. Gatti and F. De Martini, Nuclear Electronics 2, IAEA, Vienna, 1962, p. 265.
- [39] F.A. Danevich et al., Phys. Rev. C 67 (2003) 014310.
- [40] P. Belli et al., Nucl. Phys. A 789 (2007) 15.
- [41] R.B. Firestone et al., *Table of Isotopes*, 8-th ed., John Wiley, New York, 1996 and CD update, 1998.
- [42] C. Cozzini et al., Phys. Rev. C 70 (2004) 064606.
- [43] Yu.G. Zdesenko et al., Nucl. Instr. Meth. A 538 (2005) 657.
- [44] S. Agostinelli et al., Nucl. Instr. Meth. A 506 (2003) 250;  
J. Allison et al., IEEE Trans. Nucl. Sci. 53 (2006) 270.
- [45] O.A. Ponkratenko et al., Phys. At. Nucl. 63 (2000) 1282;  
V.I. Tretyak, to be published.
- [46] F.A. Danevich et al., Nucl. Instr. Meth. A 544 (2005) 553.
- [47] R. Bernabei et al., Il Nuovo Cim. A 112 (1999) 545.
- [48] M. Günther et al., Phys. Rev. D 55 (1997) 54.
- [49] G.J. Feldman and R.D. Cousins, Phys. Rev. D 57 (1998) 3873.
- [50] P. Belli et al., Nucl. Phys. B 563 (1999) 97.
- [51] Yu.M. Gavriluk et al., Bull. Rus. Ac. Sci. Physics 75 (2011) 526.
- [52] A.S. Barabash et al., Phys. Rev. C 83 (2011) 045503.
- [53] E. Andreotti et al., Astropart. Phys. 34 (2011) 643.
- [54] H. Kiel, D. Munstermann, and K. Zuber, Nucl. Phys. A 723 (2003) 499.
- [55] J.R. Wilson et al., J. Phys. Conf. Ser. 120 (2008) 052048.
- [56] P. Domin, S. Kovalenko, F. Šimkovic, and S.V. Semenov, Nucl. Phys. A 753 (2005) 337.
- [57] E.-W. Grewe et al., Phys. Rev. C 77 (2008) 064303.
- [58] I. Bikit et al., Appl. Radiat. Isot. 46 (1995) 455.
- [59] H.J. Kim et al., Nucl. Phys. A 793 (2007) 171.
- [60] A. Staudt, K. Muto, and H.V. Klapdor-Kleingrothaus, Europhys. Lett. 13 (1990) 31.

- [61] A. Bobyk, W.A. Kaminski, and P. Zareba, Nucl. Phys. A 669 (2000) 221.
- [62] J. Suhonen, Nucl. Phys. A 864 (2011) 63.
- [63] V.Yu. Denisov and A.A. Khudenko, Phys. Rev. C 79 (2009) 054614;  
Erratum Phys. Rev. C 82 (2010) 059901(E).
- [64] A.Sh. Georgadze et al., JETP Lett. 61 (1995) 882.